International Journal of Heat and Mass Transfer 51 (2008) 5486–5496

Contents lists available at ScienceDirect

International Journal of Heat and Mass Transfer

journal homepage: www.elsevier.com/locate/ijhmt

Comprehensive evaluation on the heating capacities of four typical whole body hyperthermia strategies via compartmental model

Shi-Hai Xiang [a], Jing Liu [a,b,*]

[a] Technical Institute of Physics and Chemistry, Chinese Academy of Sciences, P.O. Box 2711, Beijing 100080, PR China
[b] Department of Biomedical Engineering, School of Medicine, Tsinghua University, Beijing 100084, PR China

ARTICLE INFO

Article history:
Received 24 October 2007
Received in revised form 4 April 2008
Available online 2 June 2008

Keywords:
Whole body hyperthermia
Compartmental model
Medical instrumentation
Blood circulation
Heating efficiency
Bioheat transfer
Brain cooling
Temperature regulation
Intravascular heating
Surface heating

ABSTRACT

The whole body hyperthermia (WBH) is being regarded as a very promising way of efficiently treating patients with tumors already distributed throughout the human body. However, quite a few important issues still remain unclear, some of which are how much energy can be deposited into human body or how long will it take for a patient's body core temperature to rise from its normal to the desired point. Aiming to provide a general background for tackling the complex heat transfer behavior throughout the whole human body during a WBH treatment, we propose in this paper to adopt a compartmental model for a comprehensive evaluation of several existing typical WBH methods. The heating performance of four heating strategies such as contact-heating-based WBH (CWBH), radiative- heating-based WBH (RWBH), extracorporeal circulative-heating-enabled WBH (EWBH) as well as interventional WBH (IWBH) were compared and evaluated. The characteristics of different WBH methods were assessed in detail from the engineering perspective. Further, the effect of the thermal regulation mechanism and brain cooling upon body temperature response during WBH was investigated. Specially, this research explained for the first time the reason why intravascular heating strategies could have a higher heating efficiency in raising body core temperature than that of the heating from outside. This study would help probe into the complex behavior of the temperature response of the human body subject to various WBH. The theoretical model and calculation method could serve as a valuable guidance for future tumor treatment planning.

1. Introduction

The whole body hyperthermia (WBH) represents a promising technique capable of efficiently treating patients with distributed malignancies [1–3]. A large body of literature suggests that the therapeutic utility of WBH may generate factors that affect tumors at the molecular, cellular, tissue and organ levels. The most fundamental contributing mechanism is, perhaps, the molecular response, i.e., the loss of regulation of cell proliferation, a process thought to be controlled by apoptosis (programmed cell death) [4,5]. Hyperthermia has been found as a pathological insult that is a stimulus for apoptosis. Many studies and clinical trials have proven that WBH is rather safe and can be effective in reducing tumor size and ultimately eliminating the tumor [5]. However, the thermoregulation mechanism of a human body is so complicated, that some key parameters for WBH can still not be easily obtained through clinical experience. For example, how much energy should be deposited into the body interior and how long will it take to raise body core temperature still remains unclear up to now. According to existing literature, one can only know that the output power of various WBH equipments varies from several hundred watts to several kilowatts, and the time required for the body warming spans from dozens of minutes to hours. So far, it is still not possible to grasp the whole picture of thermal behavior of the human body via experimental measurements. For instance, one can only estimate the temperatures of the brain core or some vital organ. But these values may seriously deviate from case to case. Therefore, an appropriately justified theoretical model would provide a very useful tool to clarify these problems.

Among numerous mathematical models which have been developed to describe the heat transfer in whole body, the improved Stolwijk's 14-block model may be among the best [6–8]. It includes the human temperature regulatory mechanism and blood circulation system. Previously, this model had been adopted

* Corresponding author. Address: Technical Institute of Physics and Chemistry, Chinese Academy of Sciences, P.O. Box 2711, Beijing 100080, PR China. Tel.: +86 10 82543765; fax: +86 10 82543767.
E-mail address: jliu@cl.cryo.ac.cn (J. Liu).

0017-9310/$ - see front matter © 2008 Elsevier Ltd. All rights reserved.
doi:10.1016/j.ijheatmasstransfer.2008.04.024

Nomenclature

a, b	element of matrix in Eq. (23)
A	area (m^2)
c	specific heat (W/kg K)
C_1	intersection of the tangent of temperature curve for core
C_2	intersection of the tangent of temperature curve for muscle
$E_{b\lambda}$	spectral irradiance (W/m^3)
F	ratio in Eq. (38)
h	convective coefficient (W/m^2K)
I	radiation intensity (W/m^2)
I_0	initial radiation intensity
k_0	absorption coefficient (cm^{-1})
K	thermal conductivity (W/m K)
K_e	effective thermal conductivity (W/m K)
l	penetration depth (cm)
$m_{core,1}$	the rate of brain temperature rise at the initial stage
$m_{core,2}$	the rate of brain temperature rise at the regular stage
P_a	partial pressure of water vapour in ambient air (mmHg)
Q	heat flux (W)
Q_b	basal metabolism (W)
Q_{blood}	heat transfer to tissue by perfused blood (W)
Q_{cond}	heat transfer by conduction (W)
Q_{conv}	heat loss by convection (W)
Q_{evap}	heat loss by evaporation (W)
Q_{met}	metabolic heat production during hyperthermia (W)
Q_{radi}	heat loss by radiation (W)
Q_{resp}	heat loss by respiration (W)
r	radius(m)
T	temperature(°C)
T_b	blood temperature (°C)
V	volume (m^3)

Greek symbols

σ	Stefan-Boltzmann constant ($W/m^2 K^4$)
ε	emittance
λ	wave length (μm)
ρ	density (kg/m^3)
τ	time (s)
ω	blood perfuse rate (ml/s kg)
ω_b	basal blood perfuse rate (ml/s kg)

Subscripts

i, j	index for compartment

only for the temperature prediction in a localized hyperthermia treatment. However, few trials were made for the WBH simulation.

Traditional physical WBH methods were generally conducted through directly contacting skin with surrounding fluid. The fluid can be as either hot water (Fig. 1a), wax, air or more other flow medium. Heat is thus transferred from the surrounding fluid to the body surface via convection. A small part of the heat was then transferred from the surface to the body core through conduction in the tissue, but in large part distributed via circulating blood over the skin capillaries. This direct-immersion method is seldom utilized in clinics due to lack of efficacy in raising body core temperature and are not easy to be incorporated with chemotherapy or radiotherapy. Up to now, application of WBH in clinics has evolved into two main approaches-via infrared radiation on body surface (RWBH) (Fig. 1b) and heating blood through extracorporeal circulation (EWBH) (Fig. 1c) [9,10].

In a RWBH session, infrared radiation can penetrate skin to the superficial vascular plex which resides 1–2 mm beneath the skin and subsequently transferred heat to the patient's core. For an EWBH, a large quantity of blood is temporarily shunted to the outside of patient body, heated, and then returned to the circulation circuit where it gradually warms the rest of the human body. Recently, we proposed a novel method to realize an efficient and safe WBH, termed as interventional whole body hyperthermia (IWBH) (Fig. 1d) [11,12]. The basic principle of this method lies in that the blood is directly heated by a flexible needle inserted into the large vessel via a percutaneous (seldinger) approach. Except for its potential capability in raising body core temperature, an additional advantage of this system is its simplicity in administration and causing almost no impact on important hymodynamic parameters such as blood pressure. The EWBH and IWBH methods can be classified into a category-induced hyperthermia via heating the blood in major blood vessels. In a CWBH or RWBH therapy, the vast majority of heat is picked up by local blood perfusion and distributed throughout the body. That is, blood as a heat carrier is the same for all the above four methods. It is on the basis of this common ground, CWBH, RWBH, EWBH and IWBH can be evaluated with only one compartmental model.

2. Mathematical formulation

2.1. Compartmental model

Compartmental models are a class of theoretical formulations which have lumped parameters, in that the events in the system can be described by a finite number of changing variables. It is usually described by ordinary differential equations based on governing laws of heat and mass conservation. This is a very attractive method which ignores the spatial variation of variables in each compartment containing the lumped parameters and deals with only a single value (for example temperature in this paper) assigned to each compartment. In this way, the problem can be significantly simplified, which, however, still contains the most basic feature of the problem. As can be seen from Fig. 2, in the sense of a compartmental model, the human body is idealized as 12 body segments and a blood compartment. All these segments can be treated as cylindrical in shape for simplicity, except that the head is assumed to be spherical. Each body segment is further subdivided into four concentric layers. The thermophysical and physiological properties within each tissue block were assumed to be uniform. In addition, a compartment "I" for IWBH, "R" for RWBH, "C" for CWBH and a compartment "E" for EWBH are included in this model. Each body segment (head, neck, thorax, abdomen, two arms, two hands, two legs and two feet) are expressed by "i" ($1 \leqslant i \leqslant 12$) while four layers (core, muscle, fat, skin) in each segment is expressed with "j" ($1 \leqslant j \leqslant 4$). Therefore, the temperature for each body element can be characterized as $T(i, j)$. The geometric, anatomical and physical properties for each compartment are listed in Tables 1 and 2, respectively [14]. The basal blood flow rate for tissue and major organs were collected from many different sources [7,8,13,14].

2.2. Energy balance equation for whole body

Based on energy conservation equation and heat transfer theory, one can build up partial differential energy equations as well as their corresponding boundary conditions for each tissue block.

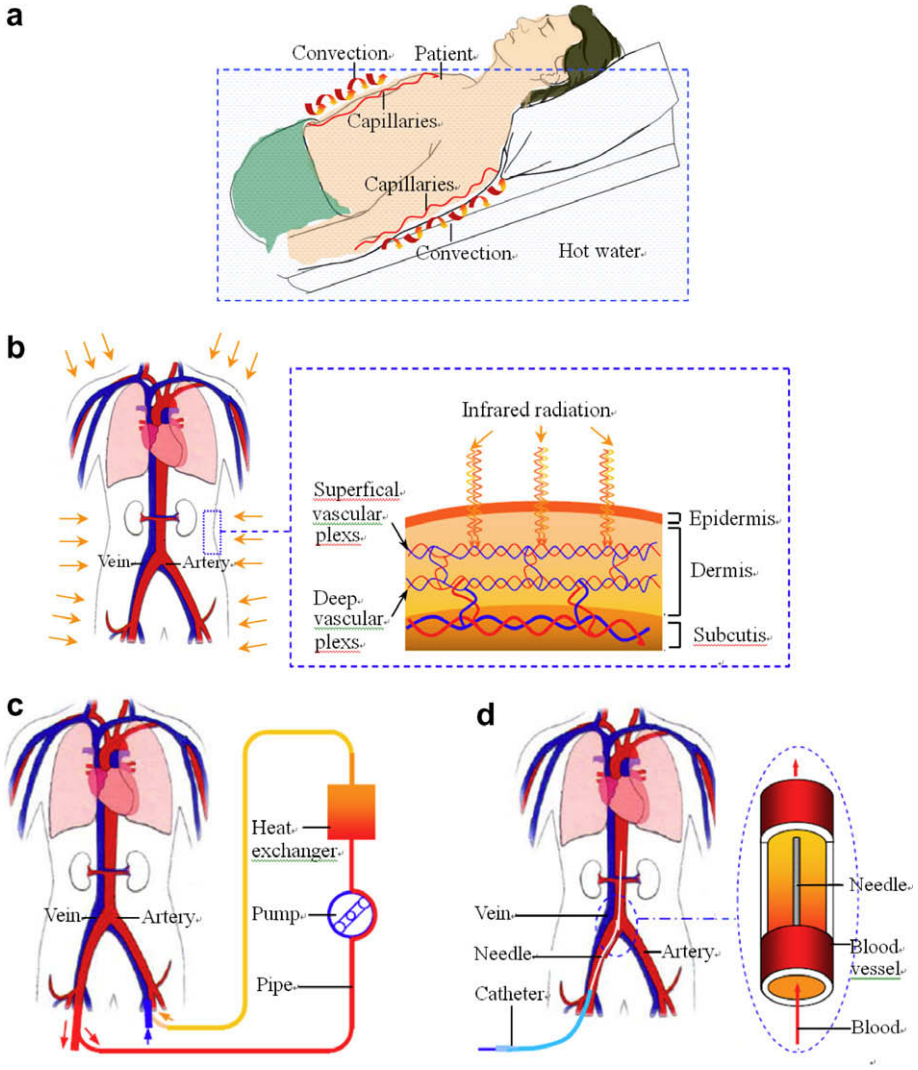

Fig. 1. Four typical approaches for realizing a WBH. (a) WBH through contact-heating method; (b) WBH through infrared radiation on body surface; (c) EWBH via heating blood from outside; (d) IWBH via directly heating blood inside vessel.

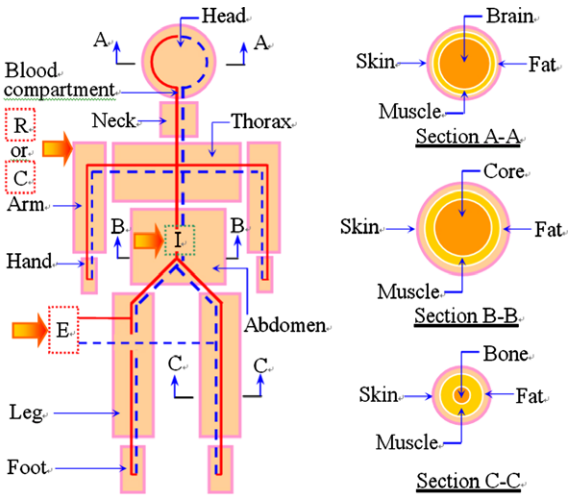

Fig. 2. Compartmental model for characterizing WBH on human body.

This consists of the mathematical model for the evaluation of temperature response during WBH therapy.

The heat exchange between different neighboring tissue blocks, or a tissue block and blood running through it can be described by the schematic diagram as shown in Fig. 3a. It is assumed that blood enters each tissue element at the same temperature.

The energy balance equations for the core, muscle, fat and skin layers of the body segment as well as the blood compartment can then be described as

Core:

$$\rho(i,j)\cdot V(i,j)\cdot c(i,j)\cdot\frac{\partial T(i,j)}{\partial\tau}=Q_{\text{blood}}(i,j)-Q_{\text{cond}}(i,j)+Q_{\text{met}}(i,j)+Q_{\text{resp}}\quad 1\leqslant i\leqslant 12,\quad j=1 \tag{1}$$

Muscle:

$$\rho(i,j)\cdot V(i,j)\cdot c(i,j)\cdot\frac{\partial T(i,j)}{\partial\tau}=Q_{\text{blood}}(i,j)+Q_{\text{cond}}(i,j-1)-Q_{\text{cond}}(i,j)+Q_{\text{met}}(i,j)\quad 1\leqslant i\leqslant 12,\quad j=2 \tag{2}$$

Fat:

$$\rho(i,j)\cdot V(i,j)\cdot c(i,j)\cdot\frac{\partial T(i,j)}{\partial\tau}=Q_{\text{blood}}(i,j)+Q_{\text{cond}}(i,j-1)-Q_{\text{cond}}(i,j)+Q_{\text{met}}(i,j)\quad 1\leqslant i\leqslant 12,\quad j=3 \tag{3}$$

Table 1
Geometrical and anatomical parameters of the model

Element	Geometric shape	Length (cm)	Diameter (cm)	Surface area (cm^2)	Material type	Volume (cm^3)	Radius (cm)
Head	Spherical	–	20.9	963	Core	1332	8.60
					Muscle	430	10.04
					Fat	335	10.25
					Skin	189	10.45
Neck	Cylinder	8.42	11.4	300	Bone	179	2.60
					Muscle	553	5.26
					Fat	86	5.56
					Skin	32	5.67
Thorax	Cylinder	28.6	25.8	2310	Core	5360	7.73
					Muscle	4324	11.30
					Fat	2899	12.64
					Skin	509	12.87
Abdomen	Cylinder	55.2	25.2	4368	Core	10595	7.82
					Muscle	7107	10.51
					Fat	7661	12.44
					Skin	717	12.60
Arms	Cylinder	127.4	8.2	3348	Bone	869	1.47
					Muscle	4701	3.73
					Fat	871	4.01
					Skin	558	4.18
Hands	Cylinder	62.0	4.6	881	Bone	195	1.00
					Muscle	268	1.54
					Fat	349	2.04
					Skin	184	2.26
Legs	Cylinder	139.3	11.4	5012	Bone	2523	2.40
					Muscle	6989	4.66
					Fat	3849	5.53
					Skin	985	5.73
Feet	Cylinder	48.4	7.2	1093	Bone	483	1.78
					Muscle	411	2.43
					Fat	819	3.36
					Skin	254	3.60

Table 2
Tissue physical properties in the models

Tissue	Density, ρ (10^{-3} kg/m^3)	Specific heat, c (10^{-3} kJ/kg · K)	Thermal conductivity, k (W/m · K)	Basal blood perfusion, ω_b (ml/s · kg)	Basal metabolism, Q_b (W/kg)
Head core	1.36	2.45	0.53	9.65	12.7
Thorax core	0.79	2.71	0.28	0.45	0.67
Abdomen core	1.10	3.35	0.55	4.12	3.83
Bone	1.30	1.59	1.16	–	–
Muscle	1.05	3.77	0.42	0.51	0.67
Fat	0.85	2.51	0.16	0.004	0.004
Skin (head, neck, thorax, abdomen, arm, hand, leg, feet)	1.00	3.77	0.21	(7.2,2.9,1.1,1.4, 1.4,3.3,1.2,2.1)	1
Blood	1.00	3.77	–	–	–

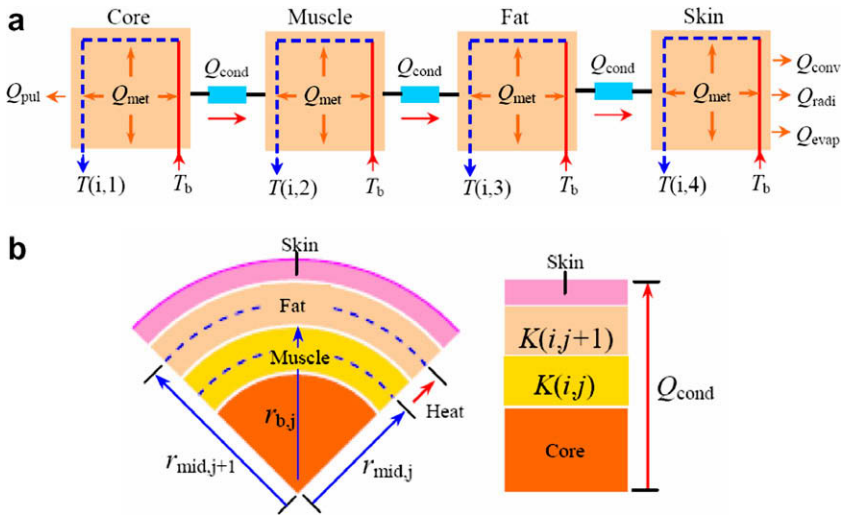

Fig. 3. Schematic for energy transport between different tissue blocks. (a) Energy balance for each tissue block; (b) heat conduction between adjacent layers.

Skin:

$$\rho(i,j)\cdot V(i,j)\cdot c(i,j)\cdot\frac{\partial T(i,j)}{\partial\tau}=Q_{\text{blood}}(i,j)+Q_{\text{cond}}(i,j)+Q_{\text{met}}(i,j)-Q_{\text{evap}}(i,j)-Q_{\text{Radi}}-Q_{\text{Conv}}\quad 1\leqslant i\leqslant 12,\quad j=4 \tag{4}$$

Blood compartment:

$$\rho_{\text{b}}\cdot V_{\text{b}}\cdot c_{\text{b}}\cdot\frac{\partial T_{\text{b}}}{\partial\tau}=\sum_{i=1}^{12}\sum_{j=1}^{4}\rho(i,j)\cdot V(i,j)\cdot\omega(i,j)\cdot\rho_{\text{b}}\cdot c_{\text{b}}\cdot(T(i,j)-T_{\text{b}})-Q_{\text{res}}+Q_{\text{in}}\quad 1\leqslant i\leqslant 12,\quad 1\leqslant j\leqslant 4 \tag{5}$$

where $\rho(i,j)$, $V(i,j)$, $T(i,j)$ and $\omega(i,j)$ are respectively the density, volume, temperature and blood perfusion rate of each tissue or organ. Q_{blood} is the heat transfer from the perfused blood to the tissue via convective heat exchange. Q_{cond} is the conductive heat exchange between different tissue layers. Q_{resp} is the heat exchange between the lung and the blood in the pulmonary system by respiration, i.e., Q_{resp} applies only to thorax core. Q_{met} is the metabolic heat production. Q_{radi}, Q_{conv} and Q_{evap} are respectively the heat loss from the skin layer to the environment via radiation, convection and evaporation. For CWBH treatment, Q_{in} is Q_{C}; for infrared radiation, Q_{in} is Q_{radi}; for the case of IWBH, Q_{in} is Q_{I}; and for EWBH Q_{in} is Q_{E}. ρ_{b}, V_{b}, c_{b} are respectively the density, volume (blood comprises approximately 7.5% of a person's total weight) and specific heat of the blood. In the following, we will discuss in detail about the expressions of Q_{blood}, Q_{cond}, Q_{conv}, Q_{radi}, Q_{evap}, Q_{resp} and Q_{met}.

2.3. Convective heat transfer between blood and tissue

Blood is an important intermediate media for heat transfer between different parts of the tissues. For WBH methods, especially for EWBH or IWBH, most of the heat is transported to the whole body owing to flow of blood. The convective heat transfer between the tissue element and the blood perfused this tissue is

$$Q_{\text{blood}}(i,j)=\rho(i,j)\cdot V(i,j)\cdot(\rho_{\text{b}}\cdot\omega(i,j)\cdot c_{\text{b}})\cdot(T_{\text{b,in}}(i,j)-T_{\text{b,out}}(i,j)) \tag{6}$$

where $T_{\text{b,in}}(i,j)$ and $T_{\text{b,out}}(i,j)$ are the temperature of blood entering the tissue or leaving the tissue, respectively. Assuming a complete thermal equilibrium between the tissue element and the blood leaving the element .

$$T_{\text{b,out}}(i,j)=T(i,j) \tag{7}$$

and that blood enters each tissue element at the same temperature,

$$T_{\text{b,in}}(i,j)=T_{\text{b}} \tag{8}$$

where T_{b} is the temperature of the blood entering each compartment. Then one gets,

$$Q_{\text{blood}}(i,j)=\rho(i,j)\cdot V(i,j)\cdot(\rho_{\text{b}}\cdot w(i,j)\cdot c_{\text{b}})\cdot(T_{\text{b}}-T(i,j)) \tag{9}$$

2.4. Heat conduction between different tissue layers

Heat conduction occurs between the body segment in both radial and axial directions. Here, for simplicity, heat is assumed to be transferred only along radial direction (Fig. 3b). Therefore, the heat conduction between two radially concentric body segments can be expressed as

$$Q_{\text{cond}}=K_{\text{e}}\cdot(T(i,j)-T(i,j+1)) \tag{10}$$

where K_{e} is the effective heat conductance between two radial adjacent tissue layers.

$$\frac{1}{K_{\text{e}}}=\frac{1}{K_{\text{e}}(i,j)}+\frac{1}{K_{\text{e}}(i,j+1)} \tag{11}$$

For cylinders

$$\frac{1}{K_{\text{e}}(i,j)}=\frac{2\pi K(i,j)L(i,j)}{\ln(r_{b,j}/r_{\text{mid},j})} \tag{12}$$

$$\frac{1}{K_{\text{e}}(i,j+1)}=\frac{2\pi K(i,j+1)L(i,j+1)}{\ln(r_{\text{mid},j+1}/r_{b,j})} \tag{13}$$

For spheres

$$\frac{1}{K_{\text{e}}(i,j)}=\frac{4\pi K(i,j)}{1/r_{\text{mid},j}-1/r_{b,j}} \tag{14}$$

$$\frac{1}{K_{\text{e}}(i,j+1)}=\frac{4\pi K(i,j)}{1/r_{b,j}-1/r_{\text{mid},j+1}} \tag{15}$$

where $K(i,j)$ and $L(i,j)$ are the thermal conductivity and length of element "i,j"; $r_{\text{b},j}$ and $r_{\text{mid},j}$ are respectively the radius at the boundary and mid-volume of element "i,j".

2.5. Heat transfer to the environment

A neutral ambient condition (30 °C, 0.1 m/s velocity, 60% relative humidity) is assumed in this paper. The heat loss through convection from the patient's skin to the air is a function of the temperature difference between the skin and the air, the convective heat transfer coefficient as well as the body surface area, i.e.,

$$Q_{\text{Conv}}(i,4)=Ah_{\text{air}}(T_{i,4}-T_{\text{air}}) \tag{16}$$

where A is the body surface, h_{air} the convective heat transfer coefficient, and T_{air} the air temperature of the ambient.

Radiant heat exchange takes place between the patient and its surroundings. The heat loss by radiation from the patient's body surface to the ambient can be estimated by Stefan-Boltzmann's law:

$$Q_{\text{radi}}(i,4)=A\varepsilon\sigma(T_{i,4}^4-T_{\text{sur}}^4) \tag{17}$$

where ε is the emissivity of the body surface, T_{sur} the surrounding temperature, $\sigma = 5.67\times10^{-8}$ W/m^2 K^4, i.e., the Stefan-Boltzmann's constant.

The heat loss via sweat evaporation (in Table 3) in a neutral ambient is obtained from the literature [14].

2.6. Respiratory heat loss

Based on the study of Fanger [15], the following expression has been found as a practical approximation for the latent respiration heat loss,

$$Q_{\text{resp}}=0.0023\cdot Q_{\text{met}}\cdot(44-p_{\text{a}}) \tag{18}$$

where p_{a} is the partial pressure of water vapor in inspired air (ambient air).

Table 3
Skin evaporation rate for each compartment

Element	Head	Neck	Thorax	Abdomen	Arms	Hands	Legs	Feet
Sweat evaporation (W)	1.44	0.23	1.75	3.29	0.93	0.35	2.2	0.48

2.7. Internal heat production

The basic metabolic rates for each body block are listed in Table 2.

3. The controlling system in body temperature regulation

There is a significant change of physiological parameters in the human body when subjected to hyperthermia, such as blood flow rate, evaporative heat loss, metabolic heat generation rate, etc. which are partially caused by the body temperature regulation mechanism which may affect the clinical result of WBH. Thus, the temperature regulation system should also be included in the modeling. So far, the controlling equation as developed by Stolwijk may be one of the best models for simulating body temperature regulation behavior. Therefore, it will be modified for the present simulation. According to some published reports, regional blood flow, sweat evaporation and metabolic rate depend on the local temperature as well as the central command [16–19] (Fig. 4). However, a general anesthesia is often used during WBH treatment in order to inhibit the central nervous system. Tranquilizers such as scopolamine combined with anesthetics plays a strong role in central inhibition and reduction of sweat evaporation [20]. Therefore, the controlling system can be simplified as the solid line in Fig. 4.

It is shown from Fig. 4 that the error signal is a key parameter for body temperature regulation. Such an error signal can be defined as

$$\mathrm{ERROR}(i,4) = T(i,j) - T_{\mathrm{set}}(i,j) \tag{19}$$

where $T_{\mathrm{set}}(i,j)$ are the normal temperatures for each compartment and they will be the resulting sets of Eq. (24). Blood flow rate to the core, muscle and fat are kept constant during modeling. The skin blood flow is doubled for every 4.5 °C increase in local temperature above the set-point temperature of the body segment.

$$\omega(i,4) = \omega_{\mathrm{b}}(i,4)\cdot 2^{\mathrm{ERROR}(i,4)/4.5} \tag{20}$$

where ω_{b} is the basal blood perfusion rate (Table 2). The rate of sweating is assumed to double for every 4 °C increase in local temperature above the set-point, i.e.,

$$Q_{\mathrm{evap}}(i,j) = Q_{\mathrm{evap},b}(i,j)\cdot 2^{\mathrm{ERROR}/4} \tag{21}$$

where $Q_{\mathrm{evap,b}}$ (Table 3) is the basal sweat evaporation. There is a non-linear increase in the metabolic rate as the body temperature increases, especially during whole body hyperthermia. Thus, the effect of local temperature on metabolic heating is included in this model.

According to Robins et al. [17], the relationship between the metabolic rate during hyperthermia and the basic metabolic rate can be expressed by the following formula,

$$Q_{\mathrm{met}(i,j)} = Q_{b(i,j)}\cdot 1.07^{\mathrm{ERROR}/0.5} \tag{22}$$

where $Q_{\mathrm{b}(i,\,j)}$ is the basal metabolic rate for each body segment.

4. Method of solution

Under a steady basal physiological state, the 49 energy balance equations (48 energy balance equations for body segments and one equation for blood compartment) are solved simultaneously under a set of thermally neutral ambient air conditions. Considering that the human body is symmetric, the temperatures for the left arm, hand, leg, and foot are then identical to that of their counterpart at the right hand side. So the 49 equations can be reduced into 33 equations. The MATLAB was applied for solving the present model by the following matrix

$$\begin{bmatrix} a_{1,1} & a_{1,2} & a_{1,3} & \cdots & a_{1,33} \\ a_{2,1} & a_{2,2} & a_{2,3} & \cdots & a_{2,33} \\ a_{3,1} & a_{3,2} & a_{3,3} & \cdots & a_{3,33} \\ \vdots & \vdots & \vdots & \ddots & \vdots \\ a_{33,1} & a_{33,2} & a_{33,3} & \cdots & a_{33,33} \end{bmatrix} \begin{bmatrix} T_{1,1} \\ T_{2,1} \\ T_{3,1} \\ \vdots \\ T_{33,1} \end{bmatrix} = \begin{bmatrix} b_{1,1} \\ b_{2,1} \\ b_{3,1} \\ \vdots \\ b_{33,1} \end{bmatrix} \tag{23}$$

Thus, one has,

$$T = a/b = \begin{bmatrix} a_{1,1} & a_{1,2} & a_{1,3} & \cdots & a_{1,33} \\ a_{2,1} & a_{2,2} & a_{2,3} & \cdots & a_{2,33} \\ a_{3,1} & a_{3,2} & a_{3,3} & \cdots & a_{3,33} \\ \vdots & \vdots & \vdots & \ddots & \vdots \\ a_{33,1} & a_{33,2} & a_{33,3} & \cdots & a_{33,33} \end{bmatrix} \Big/ \begin{bmatrix} b_{1,1} \\ b_{2,1} \\ b_{3,1} \\ \vdots \\ b_{33,1} \end{bmatrix} \tag{24}$$

The resulting sets of the 33 temperatures are the set-point temperatures (T_{set}). In order to validate the numerical code, it was necessary to compare some solutions with the typical temperature value of an internal organ and body surface as provided by classic physiological text book. Some computational results are obtained and shown in Fig. 5.

The heat transfer from the blood to the tissue is very complex such that there exists a mixture of the brain circulation and the liver circulation or renal circulation, during EWBH or IWBH therapy. In addition, different circulations require different times for completing one circulation. For example, the pulmonary circulation time is nearly 11 s while for system-wide circulation, it takes 20 s [21]. This implies that the organs close to the heart need less time for one circulation than do the organs a far distance from it,

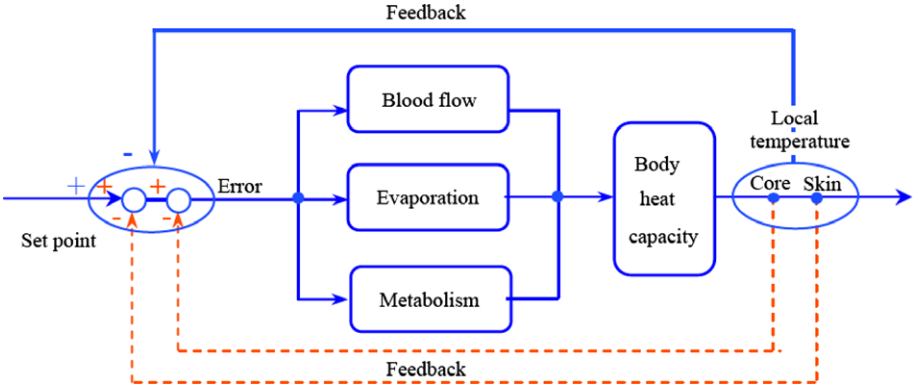

Fig. 4. The body temperature regulatory mechanism. The solid lines represent the WBH feedback model as adopted in this paper. The dashed lines represent the feedback control under cold or hot stimulus (non-WBH therapy).

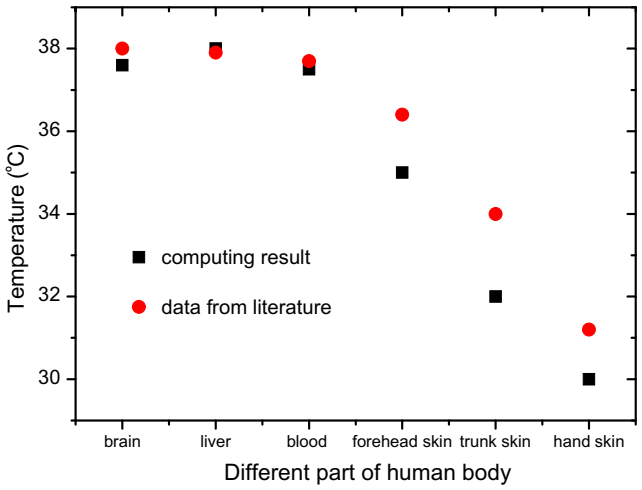

Fig. 5. Comparison between computational data and literature value.

i.e., the former's temperature increasing rate is higher than the latter. Therefore, obtaining transient temperature data in each body block is a challenging issue. Since blood is the heat carrier, and the temperature rise of the blood leads to the temperature rise of the whole body, for simplicity, the whole complex heating procedure may be separated as two simple parts. The first one is that the blood is heated, and the second is that the hot blood perfuses the tissue and the organs, which leads to the temperature increase of the whole body. Thus, the next work in this paper is to evaluate the average temperature increase of the entirety of the blood and the temperature variation of each tissue or organ.

From Eq. (5), one can have

$$\frac{\partial T_b}{\partial \tau} = \left[\sum_{i=1}^{12}\sum_{j=1}^{4}\rho(i,j)\cdot V(i,j)\cdot\omega(i,j)\cdot\rho_b\cdot c_b\cdot(T(i,j)-T_b) - Q_{res}+Q_{in}\right]\Big/(\rho_b\cdot V_b\cdot c_b) \quad 1\leqslant i\leqslant 12,\quad 1\leqslant j\leqslant 4 \tag{25}$$

Its governing equation is discretized as

$$\frac{T_b^{i+1}-T_b^i}{\Delta\tau} = \left[\sum_{i=1}^{12}\sum_{j=1}^{4}\rho(i,j)\cdot V(i,j)\cdot\omega(i,j)\cdot\rho_b\cdot c_b\cdot(T_{(i,j)}^i-T_b^i) - Q_{res}+Q_{in}\right]\Big/(\rho_b\cdot V_b\cdot c_b) \tag{26}$$

Hence

$$T_b^{i+1} = T_b^i + \left[\left(\sum_{i=1}^{12}\sum_{j=1}^{4}\rho(i,j)\cdot V(i,j)\cdot\omega(i,j)\cdot\rho_b\cdot c_b\cdot(T_{(i,j)}^i-T_b^i) - Q_{res}+Q_{in}\right)\Big/(\rho_b\cdot V_b\cdot c_b)\right]\cdot\Delta\tau \tag{27}$$

For one circulation, once the blood temperature is acquired, each body block temperature can hereafter be obtained using the similar method as above.

Core:

$$T_{(i,j)}^{i+1} = T_{(i,j)}^i + [(Q_{blood}(i,j)-Q_{cond}(i,j)+Q_{met}(i,j) + Q_{resp})/(\rho(i,j)\cdot V(i,j)\cdot c(i,j))]\cdot\Delta\tau \quad 1\leqslant i\leqslant 12,\quad j=1 \tag{28}$$

Muscle:

$$T_{(i,j)}^{i+1} = T_{(i,j)}^i + [(Q_{blood}(i,j)+Q_{cond}(i,j-1)-Q_{cond}(i,j) + Q_{met}(i,j))/(\rho(i,j)\cdot V(i,j)\cdot c(i,j))]/\Delta\tau \quad 1\leqslant i\leqslant 12,\quad j=2 \tag{29}$$

Fat:

$$T_{(i,j)}^{i+1} = T_{(i,j)}^i + [(Q_{blood}(i,j)+Q_{cond}(i,j-1)-Q_{cond}(i,j) + Q_{met}(i,j))/(\rho(i,j)\cdot V(i,j)\cdot c(i,j))]\cdot\Delta\tau \quad 1\leqslant i\leqslant 12,\quad j=3 \tag{30}$$

Skin:

$$T_{(i,j)}^{i+1} = T_{(i,j)}^i + [(Q_{cond}(i,j)+Q_{met}(i,j)-Q_{evap}(i,j)-Q_{Radi} - Q_{Conv})/(\rho(i,j)\cdot V(i,j)\cdot c(i,j))]\cdot\Delta\tau \quad 1\leqslant i\leqslant 12,\quad j=4 \tag{31}$$

The temperature responses of head, abdomen and foot with heating power (Q_{in}) as 100 W and 200 W are shown in Figs. 6–8, respectively.

5. Results

From the results as given in Fig. 5, it can be seen that the temperature of the brain, liver (liver temperature may be represented by abdominal core temperature in this model) agreed well with the data in literature [20]. While the theoretical skin temperature of the forehead, trunk and hand is a little lower than the actual value, such approximation is still generally acceptable for modeling a complex human regulatory system.

From this analysis, the temperature rise in the tissue is a function of the time and the energy level. Fig. 6 showed the brain temperature increases with the heat deposited into body as 100 W and 200 W, respectively. As can be seen from Fig. 6, obviously, there are different characteristics for curve of temperature rise at different heating stage. The slope (defined as $m_{core,1}$) of the tangent line

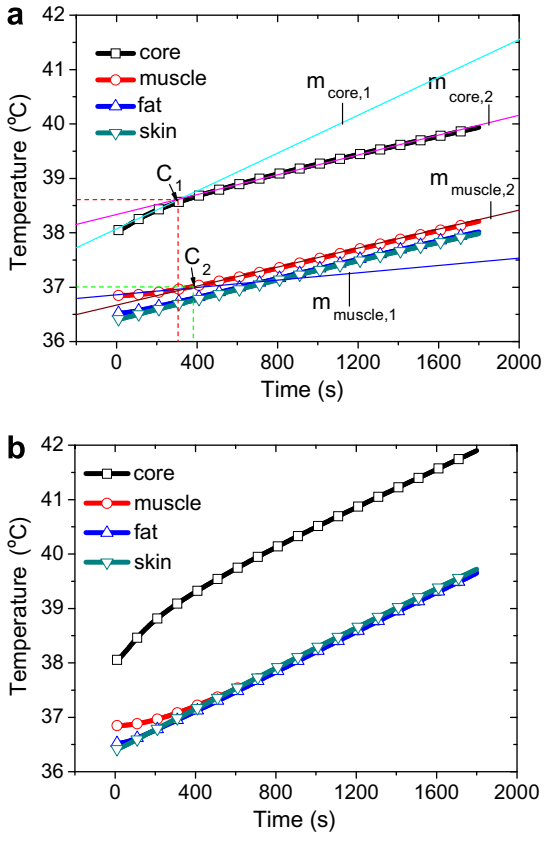

Fig. 6. Temperature response of head in WBH session. (a) 100 W energy input; (b) 200 W energy input.

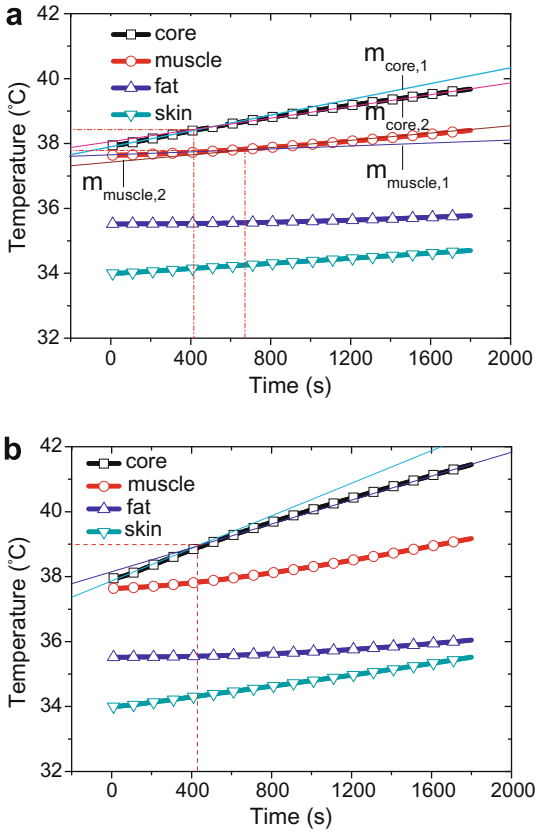

Fig. 7. Temperature response of abdomen in WBH session. (a) 100 W energy input; (b) 200 W energy input.

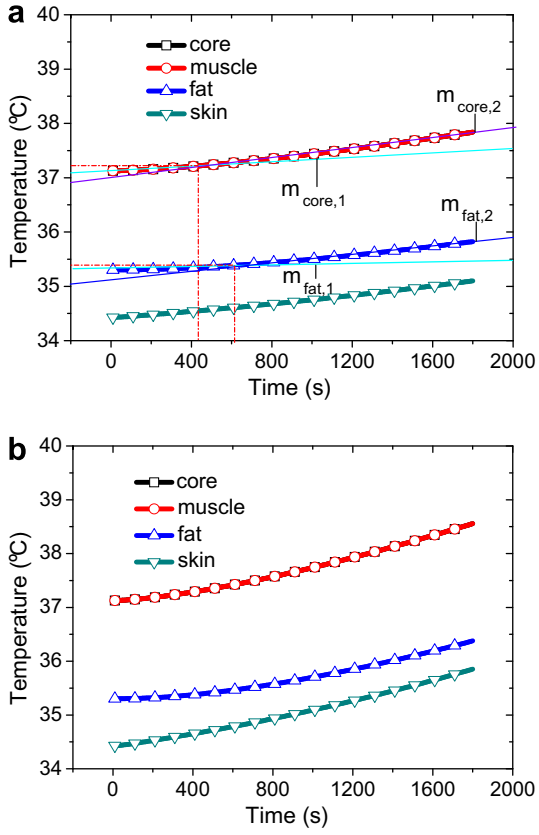

Fig. 8. Temperature response of leg in WBH session. (a) 100 W energy input; (b) 200 W energy input.

for the temperature curve for core at the starting stage (initial stage) is larger than the slope (defined as $m_{core,2}$) of the tangent line at normal heating stage (regular stage). The intersection between the tangents was defined as C_1. Also, C_1 can be taken as the clear boundary between the initial stage and regular stage. It is noted that $m_{subscript}$ defined as the slope of the temperature curve and $C_{subscript}$ defined as the intersection of the tangent line can be applied to Figs. 6–10. The reason for the above-mentioned phenomenon is that at the starting stage, the blood temperature is close to that of the tissue, i.e., there is nearly no heat transfer between blood and the surrounding tissue. Most of the energy was used to heat the blood and there is a rapid blood temperature increase in this stage. Subsequently, for the small heat capacity of brain, there is a rapid increase of the brain temperature. Next, when the temperature difference reaches certain extent (regular stage, over C_1), that will cause a full heat exchange between the blood and the tissue, the rate of temperature rise will drop slowly. But for muscle, which has a relatively larger heat capacity, situation is contrary to this. At the beginning of heating, though the muscle was perfused by the hot blood, the heat capacity of muscle is so large that the heat transferred to it cannot lead to a significant temperature increase. Accompanied by the heating progressing (over C_2 in Fig. 6), more heat is conducted from the core to muscle and metabolic rate is increasing. There will be a relatively large change in muscle temperature. From Fig. 7, one can find that the characteristic of temperature response of brain is applied to the abdomen. That is, for large heat capacity tissue such as abdominal muscle, the rate of temperature rise is "first slower" and "then faster". But for small heat capacity tissue such as abdominal core, the rate of temperature rise is "first faster" and "then slower". Fig. 7 also shows that the abdominal core, which contained most of the body's vital organs, can reach the expected temperature (40–42 °C) for killing tumors in less than 30 min. Fig. 8 gives the thermal behavior of the leg at heating. For the core of the leg composed mainly by bone, which has a low blood perfusion rate (close to zero), the temperature curve of the leg core is almost entirely in coincidence with that of the leg muscle.

6. Discussion

The theoretical approach presented in this paper provided a reasonable model to estimate the whole body temperature response when WBH therapy is used. The results reveal that net energy input larger than 100 W may meet the general clinical requirement. Here, another important question, which had never been clarified before by existing reference, needs to be answered. The question is "how much energy could be transferred into blood circulation for CWBH, RWBH, EWBH and IWBH?"

In clinics, hot water bath (43 °C) is often taken as the representative of CWBH. As mentioned in the introduction section, in a CWBH therapy, the heat transfer from surrounding fluid to the body core is a process involving a number of intermediate steps. First, heat transfer occurs by convection from the fluid to the body surface. Second, heat transfer from the body surface to the core through conduction, but in a large portion it is delivered by the skin blood flow. Since superficial capillary networks are merely 1–2 mm beneath the skin and convective heat transfer coefficient between the skin and the fluid is taken as 100 W/m^2 K, it is reasonable to ignore the conductive thermal resistance and convective thermal resistance between the fluid and the capillary. Therefore, heat transfer to the body interior through CWBH method can be expressed by the following equation:

$$Q_{CWBH} = h_{fluid} A_c \Delta T_{m,c} = h_{fluid} A_c \cdot \left(\frac{\Delta T''_{m,c} + \Delta T'_{m,c}}{2} \right) \quad (32)$$

where h_{fluid} is heat transfer coefficient of convection for fluid, here the typical value 100 W/m^2 K for water is used. $\Delta T_{\text{m,c}}$ is the arithmetic mean temperature difference between the fluid and the blood circulated in the skin capillaries. $\Delta T''_{\text{m,c}} = 43 - 42 = 1$ °C and $\Delta T'_{\text{m,c}} = 43 - 37 = 6$ °C are respectively the temperature difference at the end and initial stage of CWBH therapy. A_c is the heat transfer area between the water and the blood. Literature [24–26] suggests that the blood is uniformly distributed in the skin. A roughly estimated value for cutaneous blood content (volume fraction) is less than 10%. A_c should be $A_c = A \times 10\%$. The final solution to Eq. (32) is

$$Q_{\text{CWBH}} = 100 \times 1.8 \times 10\% \times \frac{(43-37)+(43-42)}{2} \approx 60\ \text{W} \tag{33}$$

For RWBH, as can be seen in Fig. 1a, the infrared radiation penetrates through the skin into the subcutaneous capillary network and subsequently transfers heat into the patient's core via blood circulation. The most commonly used device (closed-chamber-type) utilizes black-body radiation with a temperature of 60 °C, resulting in the emission of wavelengths of ~7 μm (infrared of very low frequency) [22]. The formulation for infrared ray attenuation along its way can be expressed as [23]

$$I = I_0 \mathrm{e}^{-k_0 l} \tag{34}$$

where I is the radiation intensity while the penetration depth is l, I_0 the initial radiation intensity, K_0 the absorption coefficient of the medium.

According to the classical electromagnetic theory, the penetration depth can be defined as

$$l = -\ln\left(\frac{I}{I_0}\right) \cdot \frac{1}{k_0} \tag{35}$$

The absorption coefficient of the skin for near-infrared radiation is 5 cm^{-1}, while for far-infrared radiation, it is 50 cm^{-1}. Thus, the penetration depth for near-infrared radiation in skin is

$$l = \frac{1}{5} = 0.2\ \text{cm} = 2\ \text{mm} \tag{36}$$

The penetration depth for far-infrared radiation in skin

$$l = \frac{1}{50} = 0.02\ \text{cm} = 0.2\ \text{mm} \tag{37}$$

Therefore, only the near-infrared radiation can be used to heating the blood circulated in the subcutaneous vascular plexs. Radiation (wavelength, $\lambda_1 - \lambda_2$) occurs according to the proportion of the total radiation energy

$$F_{b(\lambda_1-\lambda_2)} = \frac{\int_{\lambda_1}^{\lambda_2} E_{b\lambda}\mathrm{d}\lambda}{\int_0^{\infty} E_{b\lambda}\mathrm{d}\lambda} = \frac{1}{\delta T^5}\left(\int_0^{\lambda_2} E_{b\lambda}\mathrm{d}(\lambda T) - \int_0^{\lambda_1} E_{b\lambda}\mathrm{d}(\lambda T)\right) = f(\lambda_2 T) - f(\lambda_1 T) \tag{38}$$

Infrared radiation of very low frequency (0–7 μm) accounts for the proportion of the total radiation energy as

$$F_{b(0-7)} = f(333 \times 7) = f(2331) = 12\% \tag{39}$$

The results indicated that only 12% of the total energy can reach the dermis in which vascular plexs was included. As discussed above, a typical value for cutaneous blood content (volume fraction) is less than 10%. That is, the energy absorbed directly by the blood flow will be less than 2% and all the rest energy will accumulate in the epidermis and tissue. This is the reason why it is often difficult to achieve a core temperature of 42 °C without causing burn risk to the skin. Assuming that total energy emitted by the radiator is 2000 W, the energy transferred into blood circulation via RWBH should be

$$Q_{\text{RWBH}} = 2000 \times 12\% \times 10\% \approx 25\ \text{W} \tag{40}$$

Considering that some factors have been ignored in the analysis, it should be reasonable to take 50 W as the maximal heating capacity of RWBH.

The heating capacity for EWBH can be evaluated by the following simple expression

$$Q_{\text{EWBH}} = \dot{m}c_{\text{b}}\Delta T_{\text{m,e}} \approx \dot{m}c_{\text{b}}\frac{\Delta T''_{\text{m,e}} + \Delta T'_{\text{m,e}}}{2} \approx 0.5/60 \times 3770 \times \frac{8+3}{2} \approx 170\ \text{W} \tag{41}$$

where $\dot{m} \approx 400 - -600$ ml/min is the blood flow rate, $\dot{m} = 500$ ml/min is used in this study. $\Delta T_{\text{m,e}}$ is the arithmetic mean temperature difference between the inlet and outlet of the heat exchanger during EWBH, $\Delta T''_{\text{m,e}}$ is the temperature difference at the end stage of heating, its typical value is taken as $\Delta T''_{\text{m,e}} = 45 - 42 = 3$ °C. $\Delta T'_{\text{m,e}}$ is the temperature difference at the initial stage of heating, the typical value is taken as $\Delta T'_{\text{m,e}} = 45 - 37 = 8$ °C.

For IWBH, assuming that the size of power supply is 200 W, then

$$\Delta T_{\text{m,i}} = \frac{Q_{\text{IWBH}}}{\dot{m}c_{\text{b}}} = \frac{200}{3/60 \times 3770} \approx 1\ ^\circ\text{C} \tag{42}$$

where $\dot{m} \approx 3000$ ml/min is the blood flow rate in the abdominal aorta. Generally, such a small temperature difference can be achieved in IWBH. So it is reasonable to assume the heating capacity of IWBH as 200 W. In fact, we have demonstrated this opinion in our previous work [12].

Based on the heating capacity of the four typical WBH methods as discussed above, a comparison on their efficiency in raising body core temperature via compartmental model is made in Fig. 9. It is clearly seen that EWBH and IWBH are more efficient than RWBH or CWBH in elevating patient's body core temperature. CWBH and

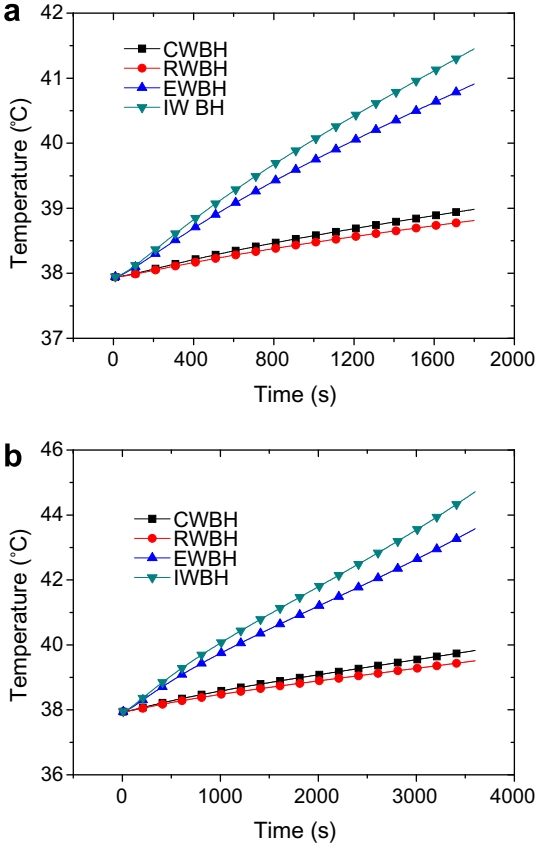

Fig. 9. Comparison on heating efficiency of four WBH methods. (a) Operation time 1800 s; (b) operation time 3600 s.

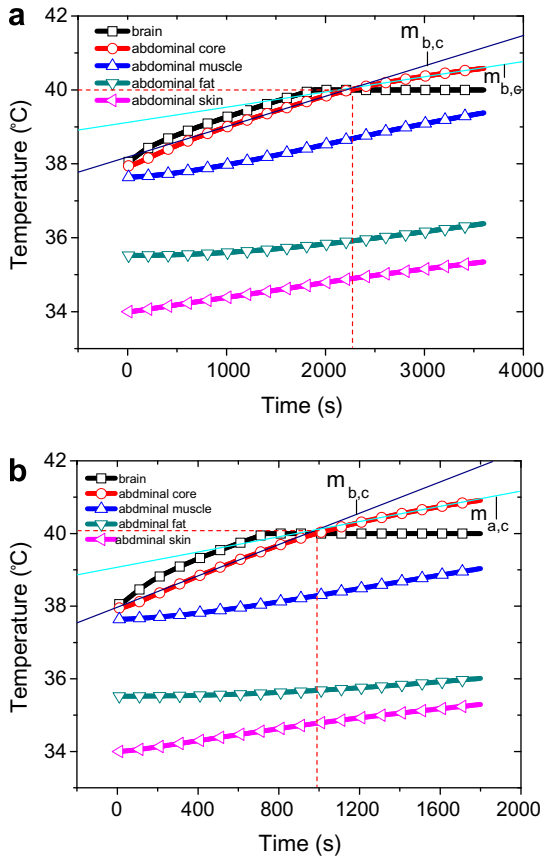

Fig. 10. Effect of brain cooling on the temperature response in WBH session. (a) 100 W energy input; (b) 200 W energy input.

RWBH have the potential to raise body core temperature. But their processes are relatively slow. This is consistent with previous clinical case report.

During the course of hyperthermia therapy, it is critical to closely monitor the brain temperature. Simple treatments such as surface cooling may be adopted to avoid the brain temperature over 40 °C. Generally, brain blood flow accounts for almost 15% of the whole blood flow. So it is necessary to examine the effect of brain cooling on the thermal response of whole body during WBH treatment. Fig. 10 depicts the effect of brain cooling upon the temperature response of the abdominal core, muscle, fat as well as skin. It is clearly seen that the brain temperature maintained at 40 °C after brain cooling and the rate of temperature rise slowed down after brain cooling ($m_{b,c}$ is the slope of the temperature rise curve before brain cooling, $m_{a,c}$ the slope of the temperature rise curve after brain cooling). This is because the blood perfused the abdomen was cooled by the blood flow in the cerebral circulation.

A more significant result as obtained in this paper was that the characteristic temperature response during WBH was revealed. Up to now, there is still no a clear ceiling to the amount of heat should be delivered to the human body for WBH. Wust et al. [27] addressed a power surplus of energy input into the human body at about 85 W to cause a systematic temperature increase of 1 °C for a patient weighing 70 kg undergo WBH. Clearly, they took the human body as an organism full of tissues such as muscle or fat, in which blood circulation is ignored. The present results revealed that the rate of temperature increase for whole body is not uniform and that the temperature increasing rate for core of internal heating is faster than body shell. From the schematic illustration in Fig. 11, one can see that the weight of body core and shell are respectively 9 kg and 46 kg (obtained from the model in Table 1). But the blood flow rate of the core is nearly three times of the body shell. According to the basic law of heat transfer, the core will be quickly heated than the shell. It is noted that the compartmental

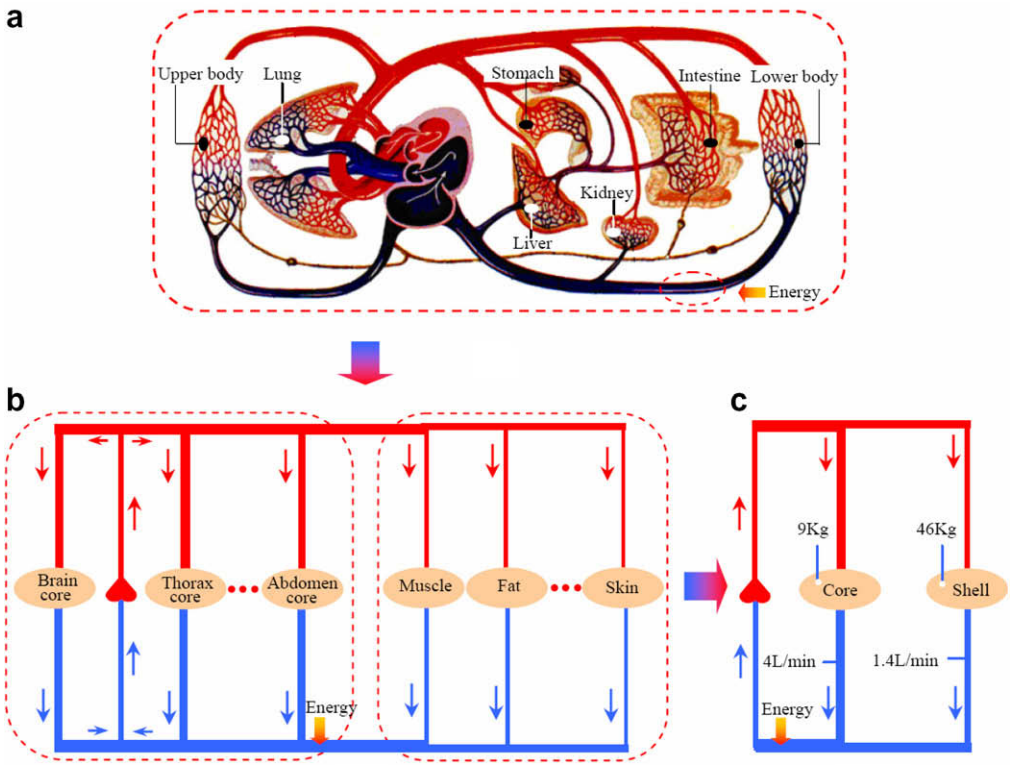

Fig. 11. Simplified schematic illustration of the blood circulation system.

model as adopted in this paper is still a simplification from the real anatomical structure, and some minor impact factors have been neglected for brevity. Though this may lower the prediction precision of the temperature response, the overall temperature variation trend as simulated still accords well to the existing data. Further, this work would be a beneficial trial for solving complex whole body bioheat transfer problem with mathematic model. Further theoretical and experimental work can be done in the near future to improve this model.

7. Conclusion

Temperature variation of the tissues and major organs during typical WBH therapy was investigated through compartmental model. The evaluation results showed that internal heating is more efficient than body surface heating. Specially, heating rate of core for internal heating is higher than that of the body surface heating owing to the heat transfer role of the blood. The body core temperature will reach the requisite value in less than 1 h provided that the net energy input into human body is 100 W. If the net energy input into human body is 200 W, the body core temperature will quickly reach 42 °C in less than a half-hour. These results could serve as a guideline to the basic and applied research for future WBH therapy.

Acknowledgement

This work is currently supported by the National Natural Science Foundation of China under Grants 50776097 and 50326022.

References

[1] E.P. Armour, D. McEachern, Z.H. Wang, P.M. Corry, A. Martinez, Sensitivity of human cells to mild hyperthermia, Cancer Res. 53 (1991) 2740–2744.
[2] A.J. Milligan, Whole-body hyperthermia induction techniques, Cancer Res. 44 (Suppl.) (1984) 4869–4872.
[3] M.M. Appenheimer, Q. Chen, R.A. Girard, W.C. Wang, S.S. Evans, Impact of fever-range thermal stress on lymphocyte-endothelial adhesion and lymphocyte trafficking, Immunol. Investig. 34 (3) (2005) 295–323.
[4] R.A. Vertrees, A. Leeth, M. Girouard, J.D. Roach, J.B. Zwischenberger, Whole-body hyperthermia: a review of theory design and application, Perfusion 7 (3) (2002) 279–290.
[5] M.T. Pritchard, S.F. Wolf, W.F. Kraybill, A.R. Elizabeth, The anti-tumor effect of interleukin-12 is enhanced by mild (fever-range) thermal therapy, Immunol. Investig. 34 (3) (2005) 361–380.
[6] J.A.J. Stolwijk, A mathematical model of physiological temperature regulation in man, NASA, 1971, CR-1855.
[7] C.K. Charny, M.J. Hagmann, A whole body thermal model of man during hyperthermia, IEEE Trans. Biomed. Eng. 34 (1987) 375–387.
[8] C.K. Charny, R.L. Levin, A three-dimensional thermal and electromagnetic model of whole limb heating with a MAPA, IEEE Trans. Biomed. Eng. 39 (1992) 836–844.
[9] M. Maeta, S. Koga, N. Shimizu, H. Kanyama, R. Hamazoe, T. Karino, T. Yamane, M. Oda, Effect of extracorporeally induced total body hyperthermia for cancer on cardiovascular function, Jpn. Heart J. 25 (1984) 993–1000.
[10] L.C. Parks, D. Minaberry, D.P. Smith, W.A. Neely, Treatment of far-advanced bronchogenic carcinoma by extracorporeally induced systemic hyperthermia, J. Thorac. Cardiovasc. Surger. 78 (1979) 883–892.
[11] S.H. Xiang, J. Liu, Y.X. Zhou, Minimally invasive whole body hyperthermia method through directly heating vessel interior (in Chinese), Beij. Biomed. Eng. 26 (5) (2007) 63–69.
[12] S.H. Xiang, J. Liu, Y.X. Zhou, X.M. Yan, Monitoring temperature of heating needle and surrounding blood during whole body hyperthermia therapy, Measure. Sci. Technol. 18 (2007) 3417–3424.
[13] L.R. Williams, R.W. Leggett, Reference values for resting blood to organs of man, Clin. Phys. Physiolog. Measure. 10 (3) (1989) 187–217.
[14] R.G. Gordon, R.B. Roemer, S.M. Horvath, A mathematical model of the human temperature regulatory system-transient cold exposure response, IEEE Trans. Biomed. Eng. 23 (1976) 434–444.
[15] P.O. Fanger, Thermal Comfort: Analysis and Applications in Environment Engineering, McGraw-Hill Inc., New York, 1972.
[16] M.J. Hagmann, R.L. Levin, Aberrant heating: a problem in regional hyperthermia, IEEE Trans. Biomed. Eng. 33 (1986) 405–411.
[17] H.I. Robins, J.P. Woods, C.L. Schmitt, J.D. Cohen, A new technological approach to radiant heat whole body hyperthermia, Cancer Lett. 79 (1994) 137–145.
[18] X.G. Yuan, Mathematical Simulation of Human Thermal Regulation System (in Chinese), Beijing University of Aeronautics and Astronautics Press, Beijing, 2005.
[19] T. Kerner, B. Hildebrandt, O. Ahlers, M. Deja, H. Riess, J. Draeger, P. Wust, H. Gerlach, Anaesthesiological experiences with whole body hyperthermia, Int. J. Hyperther. 19 (1) (2003) 1–12.
[20] T. Yao, Physiology (in Chinese), People's Medical Publishing House, Beijing, 2003.
[21] R.A. Slutsky, V. Bharqava, C.B. Hiqqins, Pulmonary circulation time: comparison of mean median peak and onset (appearance) values using indocyanine green and first-transit radionuclide techniques, Am. Heart J. 106 (1) (1983) 41–45.
[22] B. Hildebrandt, S. Hegewisch-Becker, T. Kerner, Current status of radiant whole body hyperthermia at temperature > 41.5 °C and practical guidelines for the treatment of adults, Int. J. Hyperther. 21 (2) (2005) 169–183.
[23] W.K. Lu, T.J. Li, J.Q. Zhang, Far Infrared Heating Technology (in Chinese), Shanghai Science and Technology Press, Shanghai, 1982.
[24] M.X. He, A.K. Azad, S.H. Ye, W.L. Zhang, Far-infarared signature of animal tissues characterized by terahertz time-domain spectroscopy, Opt. Commun. (259) (2006) 389–392.
[25] I.V. Meglinski, S.J. Matcher, Quantitative assessment of skin layers absorption and sin reflectance spectra simulation in the visible and near-infrared spectral regions, Physiol. Measure. 23 (2002) 741–753.
[26] C.L. Tsai, J.C. Chen, W.W. Wang, Near-infrared absorption property of biological soft tissue constituents, J. Med. Biol. Eng. 21 (2001) 7–14.
[27] P. Wust, H. Riess, B. Hildebrandt, J. Löffel, M. Deja, O. Ahlers, T. Kerner, A. von Ardenne, R. Felix, Feasibility and analysis of thermal parameters for the whole-body-hyperthermia system IRAThERM-2000, Int. J. Hyperther. 21 (1) (2005) 45–55.